

Supporting Information

Quasi-Direct Optical Transitions in Silicon Nanocrystals with Intensity Exceeding the Bulk

Benjamin G. Lee^{1*}, Jun-Wei Luo^{2,3*}, Nathan R. Neale¹, Matthew C. Beard¹, Daniel Hiller⁴, Margit Zacharias⁴, Paul Stradins¹, Alex Zunger⁵

1 National Renewable Energy Laboratory, Golden, Colorado 80401, USA

2 State Key Laboratory of Superlattices and Microstructures, Institute of Semiconductors, Chinese Academy of Sciences, Beijing 100083, China

3 Synergetic Innovation Center of Quantum Information and Quantum Physics, University of Science and Technology of China, Hefei, Anhui 230026, China

4 IMTEK, University of Freiburg, Freiburg 79110, Germany

5 Renewable and Sustainable Energy Institute, University of Colorado, Boulder, Colorado 80309, USA

Email: benjamin.lee@nrel.gov, jwluo@semi.ac.cn.

Both corresponding authors contributed equally to the paper.

I. Plasma-synthesized Si Nanocrystals:

a) Preparation

Silicon NCs are prepared using a custom-built RF-enhanced plasma reactor, the details of which have been described elsewhere¹. Briefly, 30 sccm of 10% silane (SiH_4) in helium is passed through a capacitively-coupled plasma at pressures between 2.5–3.0 Torr in a quartz reactor tube with 7 mm inner diameter and 9 mm outer diameter. Along with pressure, argon (30–80 sccm) and hydrogen (0–60 sccm) flows are adjusted to modify the residence time and tune particle size. A forward radio-frequency power of 75–100 W at 13.56 MHz is applied via an Advanced Energy Cesar 136 generator through an Advanced Energy VM1000 matching network (tuned to give a reflected power of 0–1 W) to two copper ring electrodes separated by a 1.5 cm tall ceramic spacer. An Advanced Energy Z'Scan device is used to dynamically monitor the plasma conditions and, from these measurements, it is found that 8.3–17.7 W of power is delivered to the plasma. Using the 1.5 cm spacing between the two electrodes as an estimate for the length of the plasma zone, we find particle residence times of 0.76–2.28 ms for total gas flow rates from 150–60 sccm, respectively. NCs are created in the plasma through electron impact dissociation of SiH_4 and subsequent clustering of the fragments. Hydrogen-terminated Si NCs are collected downstream from the plasma on a 400-mesh stainless steel filter and transferred via load-lock to an inert-atmosphere glove box for collection. A summary of conditions used to prepare each Si NC sample is provided in Table S1.

As-prepared, hydrogen-terminated Si NCs (~100 mg) are subjected to ligand functionalization reactions in an inert-atmosphere glove box. To the Si NC powder is added neat 1-dodecene (1.0–1.5 mL; dried by distilling from Na^0 under reduced pressure), and the suspension is heated at 220 °C in Teflon-lined, screw capped glass vials. After 10–15 min, the now dodecyl-functionalized Si NCs become soluble and deeply color the solution. Heating is continued for up to 3 h to ensure complete reaction. Ligand-capped Si NCs are purified (also under inert atmosphere) by first diluting cooled dodecene solutions with dry toluene to a volume of 10 mL and filtering the resulting toluene solutions through a 0.2 μm Nylon filter. NCs are precipitated with dry acetonitrile (10

mL for larger NCs, 30 mL for smaller NCs) and then centrifuged at 12,000 x *g* for 5 min. The supernatant is decanted, and the Si particles are dissolved in additional dry toluene (10 mL) and precipitated and isolated as before. Excess solvent is removed in vacuo, leaving dry material with the appearance of wafer Si shards (for 7.8 and 6.3 nm samples) or a waxy solid (for 3.8 and 3.2 nm samples).

b) Measurements

Transmission electron microscopy (TEM) samples are prepared inside an inert-atmosphere glove box by drop-casting a solution of dodecyl-capped Si NCs in dry hexane onto lacey-carbon-coated copper grids. Imaging is performed on a FEI Tecnai T30 microscope operating at 300 kV.

Photoluminescence measurements are made from solutions of dodecyl-capped Si NCs in 1-cm cuvettes. Emission spectra are recorded in tetrachloroethylene solutions with an optical density at the excitation wavelength of 0.2–0.4. Two systems are used to record emission spectra. Wavelengths from 535–1067 nm are recorded on a modified Horiba Jobin-Yvon Fluorolog 3 fluorescence system. Excitation at 420 nm is accomplished using a 450 W Xenon lamp, with wavelength selection provided by a double-grating spectrometer (Grating specs: 1200 grooves/mm; blazed at 500 nm), and fluorescence from the samples is detected with a liquid nitrogen-cooled CCD detector coupled to a single-grating iHR320 Imaging Spectrometer (Grating specs: 150 grooves/mm; blazed at 500 nm). Data from 800–1200 nm are collected on a QuantaMaster PTI fluorescence spectrophotometer using excitation from a Hg–Xe lamp (436 nm or 536 nm lines) passed through a monochromator and a band-pass filter. The excitation and emitted light are coupled into a light guide and routed to a monochromator. The resulting InGaAs signal is amplified using a lock-in amplifier referenced to a chopper driver, and spectra are collected by scanning the wavelength range using a monochromator. A cooled InGaAs photodiode (800–1200 nm) is used for detection. For samples with emission that spans the ranges of the two detectors, the spectra are correlated at approximately 900 nm. All spectra are corrected for the response of the detection systems.

X-ray diffraction (XRD) measurements are conducted on dry, unfunctionalized Si NCs packed into 0.5 mm glass capillary tubes and sealed with wax in an inert-atmosphere glove box (to prevent oxidation). XRD is performed using $\text{CuK}\alpha$ radiation (40 kV, 35 mA) from a Bruker D8 Discovery system equipped with a beryllium area CCD detector.

Raman spectra are recorded for dodecyl-capped NCs in cyclohexane solvent, in a backscattering configuration with excitation at 532 nm from a frequency-doubled YAG laser.

Inductively-coupled plasma optical emission spectroscopy (ICP-OES) is performed by Columbia Analytical Services, Inc., Tucson, AZ, USA.

UV-vis-NIR absorption measurements are conducted in cuvettes with 1-cm path length filled with solutions containing ~ 10 mg/mL of Si NCs in trichloroethylene (TCE). The cuvettes are sealed so there is no exposure to air. Optical transmission measurements are performed using a Varian Cary 5000i spectrophotometer equipped with an integrating sphere. Samples are placed in the path of the light beam, at the entrance of the integrating sphere.

II. Si Nanocrystals in Oxide Matrix:

a) Preparation

Size-selected Si NCs embedded in SiO_2 are deposited by the superlattice (SL) approach on quartz glass substrates². 50 $\text{SiO}_2/\text{SiO}_x$ bilayer stacks are deposited on quartz glass (GE-214) substrates by reactive thermal evaporation of SiO powder under an O_2 pressure (8×10^{-4} mbar) or high vacuum, respectively. The stoichiometry of the SiO_x is $x=1.2$, previously confirmed by Rutherford backscattering (RBS) measurements. The NCs precipitate from the Si-rich SiO_x layers which segregate into Si and SiO_2 during high temperature annealing (1100 °C) in N_2 or Ar ambient. Due to the high temperature of the anneal, the NCs are in the crystalline phase; it is also possible to produce amorphous nanoparticles when annealing at lower temperature (850 °C)³. Control over the NC diameter originates from the thickness of the SiO_x layer, which is confined between two stoichiometric SiO_2 layers. Here, the SiO_x layer is 6 nm thick. The resulting NC size,

determined by TEM analysis, is approximately 5 nm. The SiO₂ spacing layer thickness is 3 nm.

We prepare 3 different samples: one piece is annealed at 1100 °C in Ar, a second in N₂, and a third also in N₂ followed by a treatment in pure H₂ for 1 h at 450 °C. We previously established ³ that the samples have decreasing sub- and near-gap defect density in the order Ar > N₂ > N₂ then H₂. Performing absorption measurements on these 3 different samples allows us to see where there is an effect of the surface-related defects on the absorption spectra.

b) Measurements

Since the samples only have 50 layers of Si NCs, the optical absorption is quite weak, particularly near the bandedge. To detect this low amount of absorption, we employ photothermal deflection spectroscopy (PDS) ⁴, since it is sensitive to 10⁻⁴ – 10⁻⁵ levels of absorbance. For PDS, the sample is placed in a quartz cuvette containing a perfluorocarbon liquid (3M Fluorinert FC-77). The sample is illuminated with a pump beam of monochromatic light oriented perpendicular to the sample surface; the pump source consists of a tungsten filament lamp, chopped at 9.88 Hz and passed through a monochromator and reflective focusing optics. A fraction of the pump beam is absorbed in the sample, heating it and causing a thermal and refractive-index gradient in the liquid near the sample's surface. Similar to a desert mirage, the gradient in refractive index deflects a probe beam (HeNe laser); the deflection is detected by a split-diode and lock-in amplifier.

System response, including effects of source brightness and grating efficiencies, is determined using an amorphous carbon film deposited on the same type of quartz substrate. This film has a nearly flat absorption spectrum for photon energies from 0.5 to 3 eV, which we determined from transmission and reflection spectra using a Cary 6000i spectrophotometer.

PDS is also performed for bare quartz substrates that were treated by the same annealing procedures as the NC samples. The absorption of the annealed, bare quartz is spectrally flat, featureless and at least an order of magnitude lower than that of our experimental Si NC film samples, even at the lowest photon energies. Another series of

control samples is made with identical superlattice layers as the experimental samples, but not subjected to the high-temperature anneals that cause the segregation of excess Si into NCs. These suboxide superlattice control samples also have an order of magnitude lower absorption. This confirms that the observed absorption features are due to the Si NC superlattice stack, and specifically from the NCs rather than any remaining suboxide.

At higher energy, the absorption is sufficiently strong for standard spectrophotometer transmission/reflection measurements; we use a Cary 6000i system. The sample absorption data obtained by PDS is first corrected for the system response and then scaled to match the absolute sample absorption at 3 eV from spectrophotometer measurements.

Elemental analysis is done by elastic recoil detection analysis (ERDA) as described in ⁵.

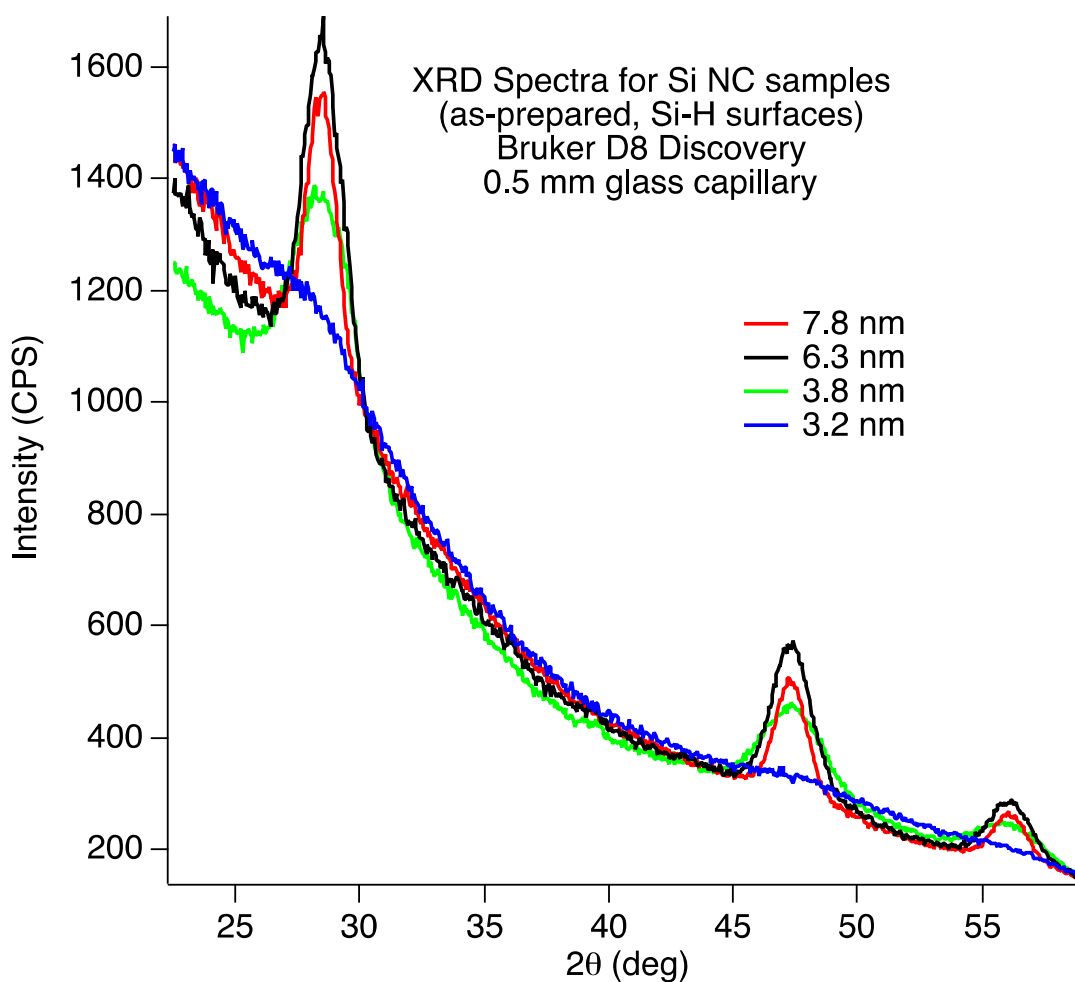
Having determined the Si content of the superlattice NC stack, we can calculate the quantitative absorption; this is shown in Fig. S2. We also plot the bulk c-Si spectrum, including the case with local field factor correction for the surrounding oxide matrix. The absorption of the NCs in oxide matrix behave nearly identical to the plasma-synthesized NCs reported in the main text of the paper. The same absorption enhancement above bulk c-Si from ~2.5 eV to more than 3 eV is seen. Second, there also doesn't appear to be any significant enhancement of the absorption near the bandedge. The difference between the 3 annealing treatments can be seen in sub- and near-gap region; here, there is slightly increased absorption in the order Ar > N₂ > N₂ then H₂ annealing treatments. This is due to the presence of surface-related defects that increase absorption, including dangling bonds, and strained bonds ³. However, the effect of surface-related defects is only in the low-energy region; at higher energies, all samples behave essentially identical.

The good agreement of optical absorption between the plasma-synthesized and oxide-matrix Si NCs strongly suggests that our observations are robust.

Table S1. Conditions used to prepare Si nanocrystals using a RF-enhanced plasma reactor.

Si Nanocrystal Size (nm)	7.8	6.3	3.8	3.2
Emission Wavelength (nm)	1000	960	840	780
Argon Flow (sccm)	30	80	60	60
10% SiH₄/He Flow (sccm)	30	30	30	30
Hydrogen Flow (sccm)	0	0	60	60
Forward RF Power Applied (W)	75	75	100	75
RF Power Delivered to Plasma (W)	9.2	8.3	17.7	10.6
Pressure (Torr)	3.0	3.0	3.0	2.5
Residence Time (ms)	2.3	1.2	0.9	0.8

Fig. S1: a) XRD of the plasma-synthesized Si NCs, showing peaks indicative of nanocrystalline phase in nanoparticles with diameters of 3.2, 3.8, 6.3, and 7.8 nm. b) Raman spectra of the NCs. The sharp peak near 520 cm^{-1} is a signature of nanocrystalline phase. We note that our separate, recent extensive study obtained better quality Raman spectra and found evidence for crystalline phase even in the smallest NCs ⁶.



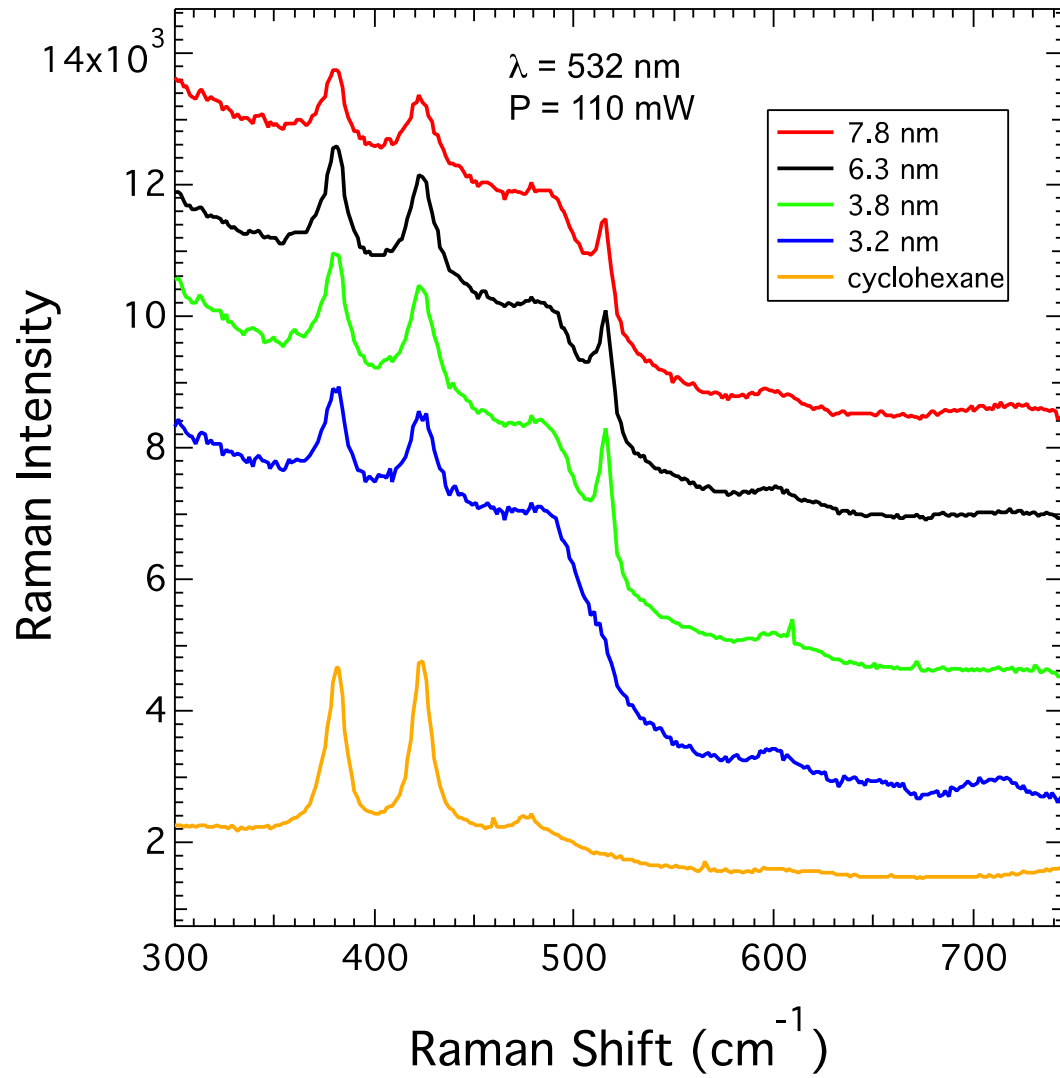
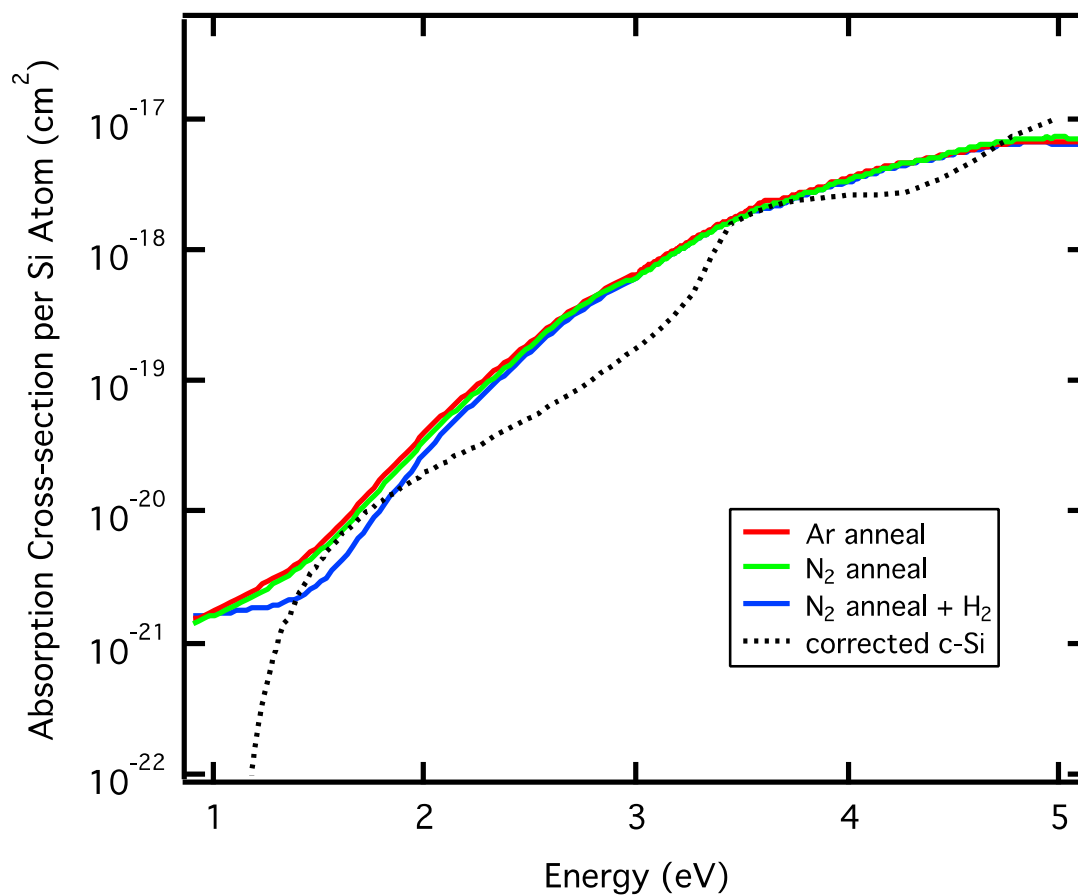


Fig. S2: Absorption cross-section per Si atom of 5 nm size Si NCs in oxide matrix with different annealing treatments, as compared to the absorption of bulk c-Si scaled to account for the local field factor correction in small particles.



References:

1. Mangolini, L.; Thimsen, E.; Kortshagen, U. *Nano letters* **2005**, 5, (4), 655-659.
2. Zacharias, M.; Heitmann, J.; Scholz, R.; Kahler, U.; Schmidt, M.; Bläsing, J. *Applied Physics Letters* **2002**, 80, (4), 661.
3. Lee, B. G.; Hiller, D.; Luo, J.-W.; Semonin, O. E.; Beard, M. C.; Zacharias, M.; Stradins, P. *Advanced Functional Materials* **2012**, 22, (15), 3223-3232.
4. Jackson, W. B.; Amer, N. M.; Boccara, A. C.; Fournier, D. *Applied optics* **1981**, 20, (8), 1333-1344.
5. Hiller, D.; Goetze, S.; Munnik, F.; Jivanescu, M.; Gerlach, J. W.; Vogt, J.; Pippel, E.; Zakharov, N.; Stesmans, A.; Zacharias, M. *Physical Review B* **2010**, 82, (19), 195401.
6. Sagar, D. M.; Atkin, J. M.; Palomaki, P. K. B.; Neale, N. R.; Blackburn, J. L.; Johnson, J. C.; Nozik, A. J.; Raschke, M. B.; Beard, M. C. *Nano Letters* **2015**, 15, (3), 1511-1516.